Divergent LIN28-mRNA associations result in translational suppression upon the initiation of differentiation

Published online 23 May 2014 *Nucleic Acids Research, 2014, Vol. 42, No. 12* ***7997–8007***
doi: 10.1093/nar/gku430

Divergent LIN28-mRNA associations result in translational suppression upon the initiation of differentiation

Shen Mynn Tan[1,*,†], Gabriel Altschuler[2,†], Tian Yun Zhao[3], Haw Siang Ang[4], Henry Yang[4], Bing Lim[1], Leah Vardy[3], Winston Hide[2,*], Andrew M. Thomson[1] and Ricky R. Lareu[5,*]

[1]Stem Cell and Developmental Biology, Genome Institute of Singapore, Agency for Science Technology and Research (A*STAR), 138672, Singapore, [2]Department of Biostatistics, Harvard School of Public Health, Boston, MA 02115, USA, [3]Institute of Medical Biology, A*STAR, 138648, Singapore, [4]Cancer Science Institute, National University of Singapore (NUS), 117599, Singapore and [5]Department of Orthopedic Surgery, NUS Tissue Engineering Program, Yong Loo Lin School of Medicine, NUS, 119228, Singapore and School of Pharmacy, CHIRI Biosciences, Curtin University, Western Australia 6102, Australia

Received February 12, 2014; Revised April 29, 2014; Accepted May 5, 2014

ABSTRACT

LIN28 function is fundamental to the activity and behavior of human embryonic stem cells (hESCs) and induced pluripotent stem cells. Its main roles in these cell types are the regulation of translational efficiency and *let-7* miRNA maturation. However, LIN28-associated mRNA cargo shifting and resultant regulation of translational efficiency upon the initiation of differentiation remain unknown. An RNA-immunoprecipitation and microarray analysis protocol, eRIP, that has high specificity and sensitivity was developed to test endogenous LIN28-associated mRNA cargo shifting. A combined eRIP and polysome analysis of early stage differentiation of hESCs with two distinct differentiation cues revealed close similarities between the dynamics of LIN28 association and translational modulation of genes involved in the Wnt signaling, cell cycle, RNA metabolism and proteasomal pathways. Our data demonstrate that change in translational efficiency is a major contributor to early stages of differentiation of hESCs, in which LIN28 plays a central role. This implies that eRIP analysis of LIN28-associated RNA cargoes may be used for rapid functional quality control of pluripotent stem cells under manufacture for therapeutic applications.

INTRODUCTION

LIN28 is an evolutionarily conserved RNA-binding protein (RBP) and a key regulator of developmental timing (1). LIN28 knockout mice showed reduction of the germ cell pool, and were are unable to survive past birth (2,3). LIN28 is highly expressed in both undifferentiated mouse and human embryonic stem cells (mESCs and hESCs) as well as developing tissues, with its expression decreasing upon differentiation (4–6). Along with key transcription factors OCT4, SOX2 and NANOG, LIN28 has been used to reprogram adult human fibroblasts to induced pluripotent stem cells (7), and was shown to be important for the maturation of these reprogrammed cells (8).

LIN28 is a predominantly cytoplasmic protein that associates with RNA in stress granules, P-bodies and polysomes (9). LIN28 also binds to the terminal loops of *let-7* miRNA family precursors and inhibits their processing into mature miRNAs (10–14). This is important in the regulation of differentiation (15,16), especially as LIN28 and *let-7* form a regulatory negative feedback loop (17). Interestingly, *let-7*-independent translation regulation by LIN28 occurs before the *let-7*-dependent step in *Caenorhabditis elegans* (18,19). LIN28 enhances translation, in a *let-7*-independent manner, of mRNAs important for cell growth in embryonic stem cells via the recruitment of RNA helicase A to polysomes (20–22). In both hESCs and somatic cells, LIN28 has also been shown to regulate splicing factor abundance (23). In mature cells, LIN28 binds to and enhances the translation of mRNAs for several metabolic enzymes, thereby increas-

*To whom correspondence should be addressed. Tel: +1 617 713 8619; Fax: +1 617 713 8621; Email: Shenmynn.Tan@childrens.harvard.edu.
Correspondence may also be addressed to Ricky Lareu. Tel: +61 8 9266 9787; Fax: +61 8 9266 2769; Email: Ricky.Lareu@curtin.edu.au.
Bioinformatics correspondence may also be addressed to Winston Hide. Tel: +1 617 432 2681; Fax: +1 617 432 5619; Email: whide@hsph.harvard.edu.
†The authors wish it to be known that, in their opinion, the first two authors should be regarded as Joint First Authors.
Present address:
Shen Mynn Tan, Program in Cellular and Molecular Medicine, Boston Children's Hospital, Harvard Medical School, Boston, MA 02115, USA.

ing glycolysis and oxidative phosphorylation, thus driving tissue repair by reprogramming cellular metabolism (24). Conversely, it was recently shown that LIN28 could also act to repress translation of endoplasmic reticulum (ER) associated transcripts (25), suggesting that post-transcriptional regulation by LIN28 could occur both positively and negatively, and thus more pervasive than previously thought.

It is unclear whether *let-7*-independent translational regulation by LIN28 occurs in hESCs upon the initiation of differentiation. RNA cargo shifting may be influenced by existing active *let-7* molecules and so *let-7*-independent regulation is defined here as the period in which mature *let-7* miRNA levels remain constant. It is also unknown what proportion of mRNAs are translationally activated or suppressed upon increased or decreased association with LIN28 during early differentiation of hESCs, and whether various differentiation cues direct early cellular changes through common and/or distinct LIN28-associated regulated pathways. Another driving force for this work was to establish a robust framework and database to analyze rapidly the functional quality of pluripotent stem cells during industrial production, as this is an essential component of the manufacturing process of cells destined for therapeutic applications.

To identify mRNAs associated with endogeneous LIN28 in hESCs, an enhanced non-cross-linking RNA-immunoprecipitation and microarray analysis technique (eRIP) was developed, as cross-linking-based protocols have been shown to introduce sequence biases and increase unspecific binding (26,27). Molecular crowding has been shown to stabilize folded RNA structure based on the principle of the Excluded Volume Effect (EVE) (28). In addition, we have demonstrated previously that the incorporation of molecular crowders into enzymatic reactions, such as real-time PCR, increases sensitivity by up to 10-fold though a number of molecular effects, including stabilizing protein-nucleic acid interactions (29). The inclusion of molecular crowders during the immunoprecipitation step of eRIP improved specificity and reduced background signal. Underscoring the sensitivity of the method, eRIPs were performed with less than a million cells per sample, 10- to 20-fold less than traditional RIP and equivalent cross-linking-based protocols (21,25). This methodology improvement also allowed multiple testing from the same small cell batch.

Analysis of the dynamic changes of LIN28 association with its target mRNAs upon the onset of differentiation of hESCs to trophoblast and neural lineages was conducted using eRIP, where the results showed consistently that the majority of these associations decrease upon short-term differentiation, prior to any change in mature *let-7* miRNA levels. Utilizing polysome loading of mRNAs as a readout for translational efficiency, we demonstrate that 95% of LIN28-associated transcripts decrease in translational efficiency within 24 h of trophectoderm-induced differentiation in hESCs. Of these, 750 increase, while 511 decrease, in LIN28 association. Crucially, the majority of these transcripts were common when a similar analysis was conducted with a neural differentiation protocol, including novel targets such as *L1TD1*, *PKM2, ID1*, *PIN1* and *CSE1L*. Gene ontology and pathway analysis reveal that LIN28 modulates cell cycle, RNA metabolism and Wnt signaling pathways through a central core of proteasomal genes for the set of 750 mRNAs, and NGF, TNF-alpha/NF-κβ and IL-2 signaling pathways for the set of 511 transcripts. We thus provide evidence that LIN28 is indeed a central regulator of stem cell pluripotency and differentiation, independent of *let-7*a miRNA regulation.

MATERIALS AND METHODS

Cell culture

H1 hESCs (Wicell) were cultured on Biomatrix in feeder-free culture conditions with mouse embryonic fibroblast-conditioned media (MEF-CM) (Tan *et al.*, submitted for publication). Briefly, human embryonic stem medium [80% Dulbecco's modified Eagle's medium-Ham's F-12 medium, 20% Knockout serum replacement (Invitrogen), 1 mM L-glutamine, 0.1 mM β-mercaptoethanol, 1% nonessential amino acids and 4 ng/ml human basic fibroblast growth factor (bFGF)] was incubated with mitomycin C-inactivated MEFs overnight, with an additional 4 ng/ml of bFGF before hESC feeding. Cultures were passaged every 5–7 days, before they became confluent. Differentiation was induced via the addition of specific factors into MEF-CM, along with the removal of bFGF. For trophoblast induction, cultures were incubated in MEF-CM with 100 ng/ml of recombinant BMP4 (R&D Systems) and 20 μM of FGFR-inhibitor SU5402 (Calbiochem) for 1–5 days (30). For retinoid differentiation, cultures were incubated in MEF-CM with 10 μM of synthetic retinoid EC23 (Reinnervate) for 1–5 days (31).

Quantitative real-time PCR

RNA was extracted from biological triplicate samples using a combination of Trizol lysis (Invitrogen) and the RNeasy kit (Qiagen). 100–500 ng of RNA from each sample was reverse transcribed using the high capacity cDNA reverse transcription Kit for mRNA analysis, or the TaqMan miRNA reverse transcription kit for miRNA analysis (ABI). All PCR reactions were performed in technical duplicates and biological replicates using validated TaqMan gene expression assays as per manufacturer's instructions on the 7900HT fast real-time PCR system (both ABI). Expression data were normalized to GAPDH (for mRNAs) or RNU6B (for miRNAs) expression levels for each sample.

siRNA transfection

siRNA transfection was performed as described previously (32). Briefly, 1×10^5 hESCs in suspension were transfected using DharmaFECT2 (Dharmacon), with 50 μM of either non-targeting siRNA control or ON-TARGETplus SMARTpool siLIN28 (both Dharmacon) as per manufacturer's recommendations, and plated onto 12-well tissue culture plates. Protein expression was analyzed 72 h after transfection.

Western blots

Protein extraction and western blots were performed as described previously (33). Briefly, cells were lysed in RIPA

buffer and cleared. Proteins were analyzed by SDS-PAGE (Invitrogen), transferred to nitrocellulose membranes and probed with the following antibodies: LIN28 (Protein Tech), PKM2 (Novus Biologicals), EZR, ACTB, KPNA2, PNP and DNMT3B (all Santa Cruz).

Microarrays

HT-12 v3.0 Beadchip microarrays (Illumina) were used for both eRIP and polysome experiments. cRNA libraries were prepared (Ambion) and samples hybridized to Beadchips (Illumina) using standard manufacturer's protocols. Data were extracted with BeadStudio software (Illumina), following quantile normalization across all samples.

Polysome fractionation

Polysomes were isolated as previously described (34,35). Cells were incubated with 100 μg/ml cyclohexamide for 10 min prior to harvesting. Ten million cells were harvested using accutase and resuspended in 10 mM Tris-HCl at pH 7.4, 10 mM NaCl, 15 mM $MgCl_2$, 200 μg/ml cycloheximide, 200 μg/ml heparin and 2000 U/m RNasin. Cells were then lysed in 0.5% Triton X-100, 1% Tween-20, 0.5% deoxycholate. Lysates were incubated on ice for 10 min and nuclei were removed by centrifugation at 12 000 × *g* for 10 min. Equal OD units were loaded onto linear 10–50% sucrose gradients (in 10 mM Tris-HCl at pH 7.4, 75 mM KCl, 1.5 mM $MgCl_2$) and centrifuged at 36 000 rpm for 2 h at 8°C in an SW41 rotor (Beckman Coulter). A piston gradient fractionator (BioComp Instruments) was used to collect twelve 1 ml fractions. Fractions were incubated with 1% SDS and 120 μg of proteinase K (Invitrogen) for 30 min at 42°C. Fractions 1–5, 6–8 and 9–11 were combined as groups 1, 2 and 3, respectively. Unfractionated cytoplasmic RNA and polysomal RNA groups were purified with phenol chloroform extraction, followed by purification on an RNeasy column with on-column DNase digestion. Poly(A) spike-in RNAs (Ambion) were added to each group of RNA. 300 ng of RNA from each group was used for microarray analysis.

Polysome microarray analysis

The hybridization intensities were first background subtracted. A two-way normalization was then performed. First, a scaling factor was obtained from spike-in controls to normalize the intensities between each polysomal group. Next, normalization was performed among the four replicates. For total RNA, the hybridization intensities were background subtracted and normalized using the cross-correlation method (36).

Excluded volume effect RNA immunoprecipitation (eRIP)

Cross-linking-free RNA immunoprecipitation was performed as previously detailed (27), with the addition of a cocktail of molecular crowders [2.5 mg/ml Ficoll PM400, 7.5 mg/ml Ficoll PM70 (both GE Healthcare) and 250 ng/ml Dextran Sulphate 670k (Fluka)] to the immunoprecipitation step. Briefly, 10 μl of antibody [LIN28 (Protein-Tech) or U1 (Santa Cruz)] was incubated with BSA-blocked Protein G sepharose beads (Sigma) overnight, washed five times with NT2 buffer, and resuspended in 850 μl of NT2 buffer with molecular buffer cocktail and 200 U of RNase Out and 100 U of SUPERase IN (Life Technologies). Human ESC cultures that were 50–70% confluent (1–5 × 10^6 cells) were then washed with phosphate buffered saline (Invitrogen) and lysed with 500 μl of polysome lysis buffer. Nuclei were removed by centrifugation at 5000 × *g* for 5 min. 100 μl of the cytoplasmic lysate was then added to 900 μl of antibody-coated bead slurry from above for each sample, and rotated at 4°C overnight. The next day, beads were washed five times with NT2, and the RNA eluted with Trizol reagent (Invitrogen), followed by standard RNA precipitation protocols. The RNA was resuspended in 50 μl of RNase-free water and ready for either real-time PCR or microarray analysis, where volumes were kept constant across all samples. 10 μl of RNA was used for each sample for preparation of cRNA for microarray analysis.

LIN28 eRIP microarray analysis

Samples were analyzed in biological triplicate for all four experimental conditions; untreated, ligand-induced trophoblast lineage differentiation protocol (TE) at 12 h, TE at 24 h, and ligand-induced neuronal lineage differentiation protocol at 24 h. Samples were quantile normalized across the full dataset, the quality of the microarray data was assessed using BeadStudio software (Illumina) and the similarity of the replicates verified by unsupervised hierarchical clustering. A single outlier array was detected and excluded from the subsequent analysis. A T-test was used to compare the gene expression levels from the LIN28 and U1 control eRIP microarrays, and a *p*-value cutoff of 0.01 was applied. Probes were also filtered by the eRIP fold change. To determine an appropriate fold change cutoff the eRIP false positive rate was estimated at discrete cutoff levels between 0.5 and 3 from the number of probes binding to the U1 control eRIP. Increasing the cutoff reduced the false positive rate until a fold change of 2, corresponding to a false positive rate of approximately 1.75%, after which only a small decrease was observed, and so a 2-fold cutoff was used for the analysis of the LIN28-eRIP.

LIN28 eRIP timecourse analysis

The change in LIN28 binding over the trophoblast lineage differentiation timecourse was quantified using a linear fit to the LIN28 versus U1 control eRIP fold change across the three time-points, using all experimental replicates. A scaled gradient was defined as the LIN28 gradient divided by the standard error in the gradient. An equivalent neuronal lineage differentiation gradient was determined but, as there are only two neuronal-differentiation time-points, no scaled gradient was defined.

Pathway enrichment analysis and network visualization

For each of the LIN28 gene lists a *p*-value of over-representation in a suite of canonical pathways (KEGG, Wikipathways and Reactome) was determined using the hypergeometric distribution. A visualization of the physical

interactions between the LIN28-bound transcripts in the top five enriched pathways was rendered using the Genemania plugin (37), within Cytoscape software (38).

Analysis scripts

The R scripts used to conduct the microarray analysis and compile the associated figures in this manuscript have been compiled as a Sweave file, available as supplementary information.

Accession numbers

LIN28 eRIP and polysome microarray datasets are available in the ArrayExpress database (www.ebi.ac.uk/arrayexpress) under accession numbers E-MTAB-1652 and E-MTAB-1653, respectively.

RESULTS

Characterization of differentiating hESCs

The initial 24 h of defined directed differentiation of hESCs was used to investigate the dynamic interactions of endogeneous LIN28 with its target mRNAs during the initiation of differentiation. Two distinct established differentiation protocols were used, rather than random differentiation via embryoid body formation. Trophectoderm (TE) differentiation was induced by the addition of BMP4 and FGFR-inhibitor SU5402 (30), and neural (N) differentiation induced by synthetic retinoid EC23 (31). Within 24 h of directed differentiation of H1 hESCs, transcript expression of early trophectoderm markers *FGFR3* and *CDX2* increased dramatically only in cells treated with the TE differentiation protocol. An increase in the expression of neural markers *PAX6* and *SOX9* was detected only for cells treated with EC23 (Figure 1A). Both differentiation protocols induced a 50% decrease in mRNA levels for pluripotency markers *NANOG* and *SALL4* within 24 h. However, no change was detected for *OCT4* and *LIN28* transcripts upon differentiation (Figure 1B). The levels of mature *let-7* miRNAs and *miR-10a* remain unchanged in the first 24 h of differentiation (Figure 1C). Conversely, levels of *miR-296* increased as has previously been shown upon retinoid differentiation (33). These results are consistent with established data for induced differentiation of hESCs and with the previous findings that LIN28 expression decreases, and mature *let-7* expression increases, only after 5–10 days of embryoid body differentiation in hESCs (11).

Establishing quality of LIN28 eRIP and polysome profiling

We previously employed the concept of EVE to dramatically improve the specificity and sensitivity of real-time PCR (29). Here we expand the utility of EVE in a non-crosslinking RNA-immunoprecipitation (RIP) protocol (27), which we term eRIP. The eRIP method introduces neutral and hydrophilic macromolecular crowders during the immunoprecipitation step to more closely emulate the intracellular biophysical environment and reduce method-induced deviations in molecular interactions, as well as maximize the capture efficiency and specificity of antibody-RBP-RNA complexes from hESC cytoplasmic extracts. Western blot analysis of LIN28 protein in the immunopricipitate and flow-through from conventional RIP compared to eRIP indicated that antibody-LIN28 affinity was enhanced in eRIP (Figure 1D), illustrating the improved efficiency of our method. Illumina beadchip microarray analysis was performed on H1 hESC total RNA and eRIPs with beads only and anti-U1 negative controls, and anti-LIN28, versus treatment types: untreated cells, neural differentiation for 24 h (N24) and trophectoderm differentiation for 12 and 24 h (TE12 and TE24). eRIP enrichment values for all LIN28-associated genes were generally correlated between the two differentiation protocols at 24 h, with an R^2 value of 0.59, suggesting that LIN28-mediated post-transcriptional regulation is involved in the initiation of both differentiation programs (Figure 1E). Unsupervised hierarchical cluster analysis of this dataset demonstrated that each sample set clustered together distinctly with itself, where the transcript representation profile for each treatment of each sample was similar (Figure 1F). Importantly, the beads only and U1 negative controls all clustered together with a similar pattern indicating coherent and reproducible background control. As such, the method was deemed fit for use for research purposes, but has yet to be qualified to ICH guidelines. It is interesting to note here that the neural and trophectoderm eRIP patterns were similar in all replicates. Similar relative patterns were also observed in all total RNA samples, suggestive that many, but not all, mRNA levels do not alter significantly within the first 24 h of hESC differentiation and that modulation in translational efficiency may be a key factor in early differentiation responses.

Transcripts significantly associated with LIN28 were identified by differential expression analysis (39), comparing LIN28 and U1 eRIP arrays (Figure 2A). A total of 1984 transcripts were significantly associated with endogeneous LIN28 in undifferentiated hESCs (Figure 2B and Supplementary Table S1). A recent study demonstrated that LIN28 binds selectively to quadruplex-forming G-rich RNA sequences (QGRS) (O'Day *et al.*, submitted for publication). To substantiate and endorse this gene list, we compared the QGRS G-score per kb (40) for the top 50 LIN28-associated mRNAs detected herein with the top 50 LIN28-associated mRNAs detected by two comparable studies (21,41), and the top 50 mRNAs associated with G-quartet-binding FMRP as a positive control (42). As negative controls, a randomly generated list of 50 mRNAs (RSA-tools, http://rsat.ulb.ac.be/random-genes_form.cgi) and the top 50 mRNAs associated with the AU-rich binding HuR were used (43). A cumulative frequency plot of these data confirms that all three of the LIN28-associated datasets are significantly enriched for G-rich, quadruplex-forming sequences, with Kolmogorov-Smirnov (K-S) test p-values of < 0.05 compared to the random gene list (Figure 2C). While it can be challenging to directly compare across different studies due to methodological differences, such as IP protocol, cross-linking and capture of endogeneous versus exogeneous LIN28 in different cell lines, eRIP did identify 53% of the 276 high-confidence targets in the study, by Peng *et al.*, which captured exogeneous FLAG-tagged LIN28 via

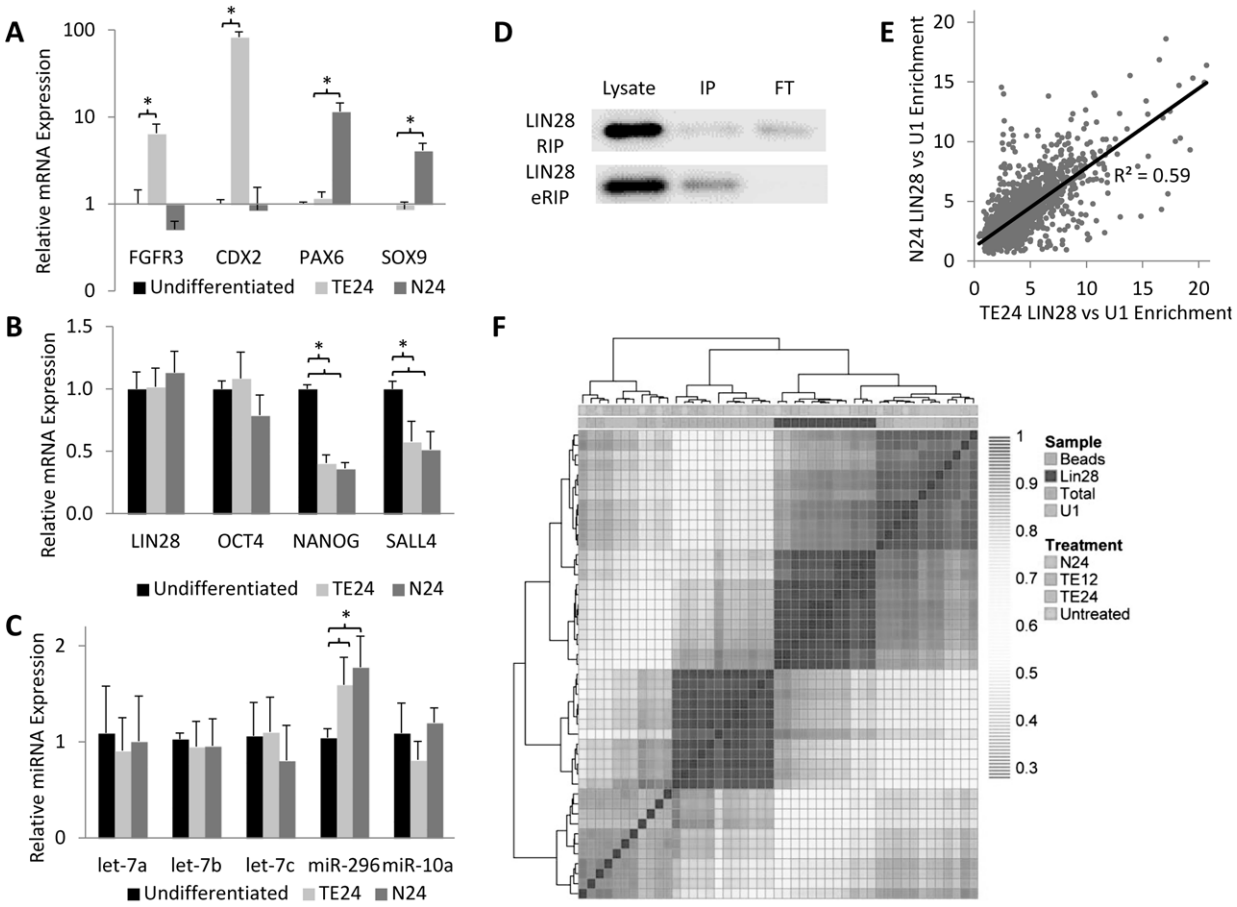

Figure 1. Analysis of 24 h trophectoderm (TE24) and neuronal retinoid (N24) differentiation. Quantitative real-time PCR expression analysis of (**A**) differentiation markers, (**B**) pluripotency markers and (**C**) miRNAs comparing hESCs induced to differentiate with either TE24 or N24 to undifferentiated cells. Trophectoderm markers *FGFR3* and *CDX2* were only upregulated upon TE24 treatment, while *PAX6* and *SOX9* were only upregulated upon N24 treatment. *NANOG* and *SALL4* were downregulated, whereas *LIN28* and *let-7* levels remained unchanged with both differentiation protocols. (**D**) Western blot of LIN28 protein levels in cytoplasmic lysates, 5-fold-diluted immunoprecipates (IP), and 10-fold-diluted first flow-throughs (FT) for conventional RIP compared to enhanced RIP (eRIP), illustrating the increased efficiency of eRIP. (**E**) Comparison of LIN28-enriched genes for both TE24 and N24 differentiation treatments, showing a correlative R^2 value of 0.59. (**F**) Unsupervised hierarchical clustering of Illumina beadchip microarrays showing differences between control (beads-only and U1 nuclear RBP) eRIPs, LIN28 eRIPs and total RNA expression profiles. Error bars depict the S.D. of three independent experiments. (*$p < 0.05$).

non-cross-linking RIP in H1 hESCs (21). Forty-five percent of eRIP targets were also identified in the Wilbert *et al.* study, which used cross-linking IP (CLIP) to capture endogeneous LIN28 in H9 hESCs (23). Twenty-four percent of 1803 LIN28-associated genes observed by Hafner, where photoactivatable-ribonucleoside-enhanced CLIP was used to capture exogeneous LIN28 in HEK293 cells (41), were identified by eRIP. Overall, eRIP data show a higher correlation with non-cross-linking RIP methodology used to identify endogeneous LIN28-associated mRNAs. In addition, 50% of the LIN28-associated transcripts identified herein are novel and not present in any of the three previously published datasets. These data may reflect the broader spectrum of potential LIN28 targets whose association with LIN28 may vary across cell types due to differences in aspects such as dynamic balances of RNAs (including small non-coding RNAs) and other RBPs, as well as phosphorylation/acetylation states of the endogeneous protein.

Genome-wide polysome profiling is an established indicator of translational efficiency, where greater association of mRNA with polysomes is an indicator of increased translation efficiency, and vice versa (34,44). This was applied to explore the translational regulatory landscape of these hESCs and how this related to LIN28-associated transcripts. Polysomal fractions were separated into four distinct groups and the translational efficiency of each transcript was computed as a ratio of the microarray signal from heavy to light polysomes (or G3 to G2) (Figure 2D and Supplementary Table S2). This can be visualized in a Q-Q plot comparing experimental to theoretical T-scores (Figure 2E), which is distinctly different from the LIN28-association plot in Figure 2A, where we did not detect much enrichment in the negative direction (i.e. for U1-association). To substantiate the microarray dataset, quantitative real-time PCR was performed for 12 randomly selected mRNAs across all of the gradient groups, and both datasets were highly correlated ($R^2 = 0.83$) (Figure 2F).

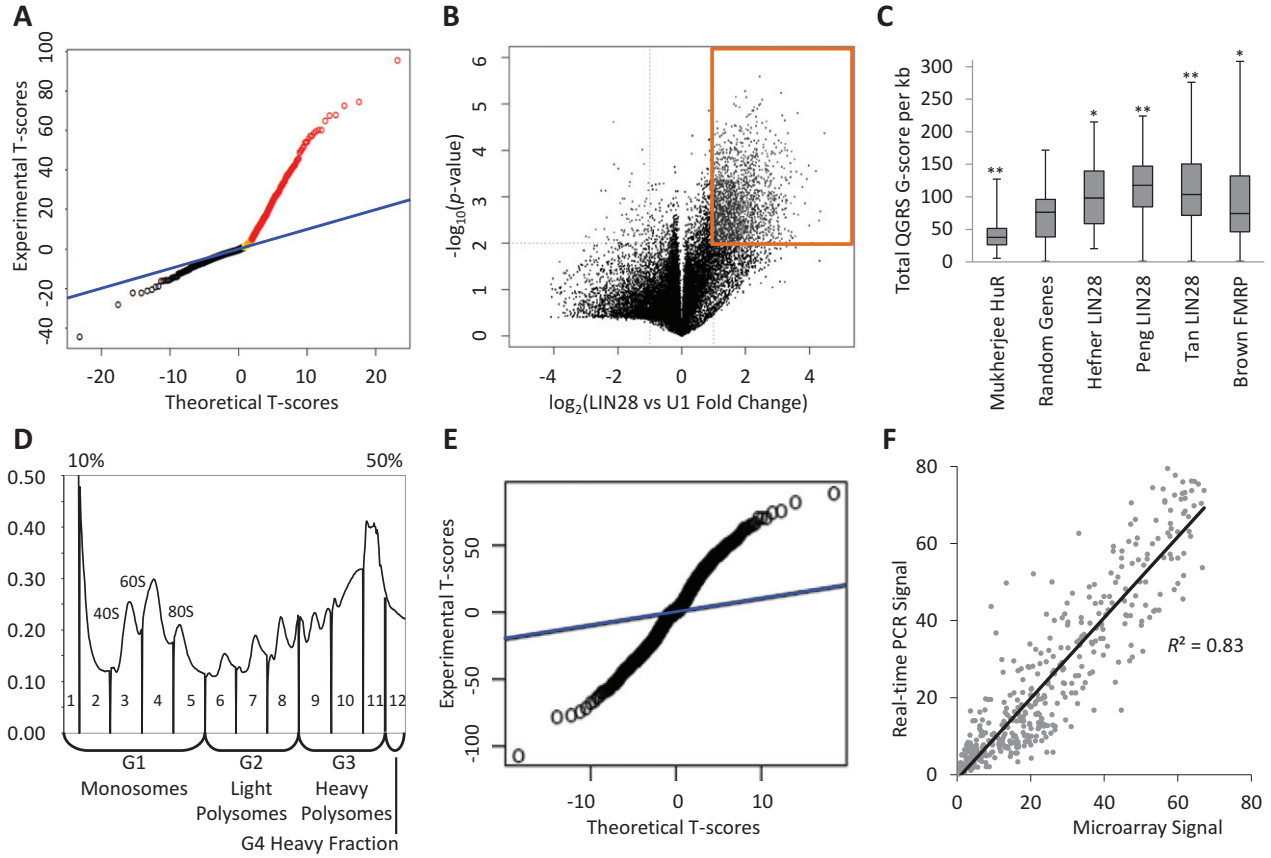

Figure 2. Analysis of LIN28 eRIP and polysome profiling. (**A**) Q-Q plot comparing the experimental and theoretical T-scores for LIN28 compared to U1 eRIPs in untreated hESCs. Data points above and below the blue line represent mRNAs that deviate from the expected distribution, where positive scores represent LIN28 compared to U1 RIP enrichment and vice versa. T-scores above 1 (yellow), 2 (orange) and 5.841 (red, equivalent to a *p*-value of <0.01) are highlighted. (**B**) Volcano plot illustrating the relationship between *p*-value and fold change for LIN28 compared to U1 eRIPs. Of the mRNAs that have a *p*-value of <0.01, 1,984 have a fold enrichment value of >2 (orange box), suggesting that these mRNAs are associated with LIN28 in undifferentiated hESCs. (**C**) Box plot of the total quadruplex-forming G-rich RNA sequences (QGRS) score per kb of the top 50 transcripts associated with various RNA-binding proteins. Compared to an RSA-generated random list of 50 genes, FMRP and all LIN28 datasets were enriched for such sequences, but HuR, known to target AU-rich regions, was not. ** indicates a K-S test p-value of < 0.01, and * p-value < 0.05, compared to the list of random genes. (**D**) Schematic of representative spectra for the polysome analysis experiments, showing the 12 fractions collected and how they are grouped for microarray analysis. (**E**) Q-Q plot of the translational efficiency ratio (calculated as the ratio of G3:G2) for undifferentiated hESCs. Data points above and below the blue line represent mRNAs that deviate from the expected distribution, where positive scores represent highly efficiently translated mRNAs and vice versa. (**F**) Quantitative real-time PCR validation of the polysome microarray data for 12 random genes, resulting in a correlative R^2 value of 0.83.

LIN28 association and translational efficiency upon hESC differentiation

Considering all three time-points and both differentiation protocols, 2995 transcripts were significantly associated with LIN28 in at least one time point (Supplementary Table S1). To identify and compute changes at the onset of differentiation, we calculated the timecourse gradient of total mRNA expression, LIN28 association, and translational efficiency for each transcript across the three time-points: untreated (or undifferentiated), 12 h TE and 24 h TE treatment. A positive gradient value indicates an increase in a particular observation, such as LIN28 association, upon 24 h of hESC differentiation into the trophectoderm lineage. We defined the scaled gradient as the ratio of the gradient to the standard error of the gradient. Transcripts with scaled gradients between −1 and 1 (i.e. that the magnitude of the standard error is greater than the gradient) were disregarded from this part of the analysis.

We compared the change in transcript expression during trophoblast differentiation of the LIN28-associated transcripts identified in this study, the significant LIN28 targets from the Peng study (21), known trophectoderm and pluripotency genes (45), and all expressed genes (Figure 3A). As expected, transcript levels of trophectoderm marker genes significantly increased upon TE differentiation, while transcript levels of pluripotency-related genes significantly decreased. The LIN28-associated transcripts from both datasets showed little change, demonstrating that these genes were not co-regulated at the transcriptional level. When the change in translational efficiency was compared for the same lists of genes, only the LIN28-associated transcripts from this study showed a significant decrease in translational efficiency upon differentiation (K-S test p-value < 0.001) (Figure 3B), supporting our hypothesis that LIN28-associated transcripts are regulated at the post-transcriptional level. The majority of transcripts (750, or 56% of LIN28-associated transcripts) decreased in both

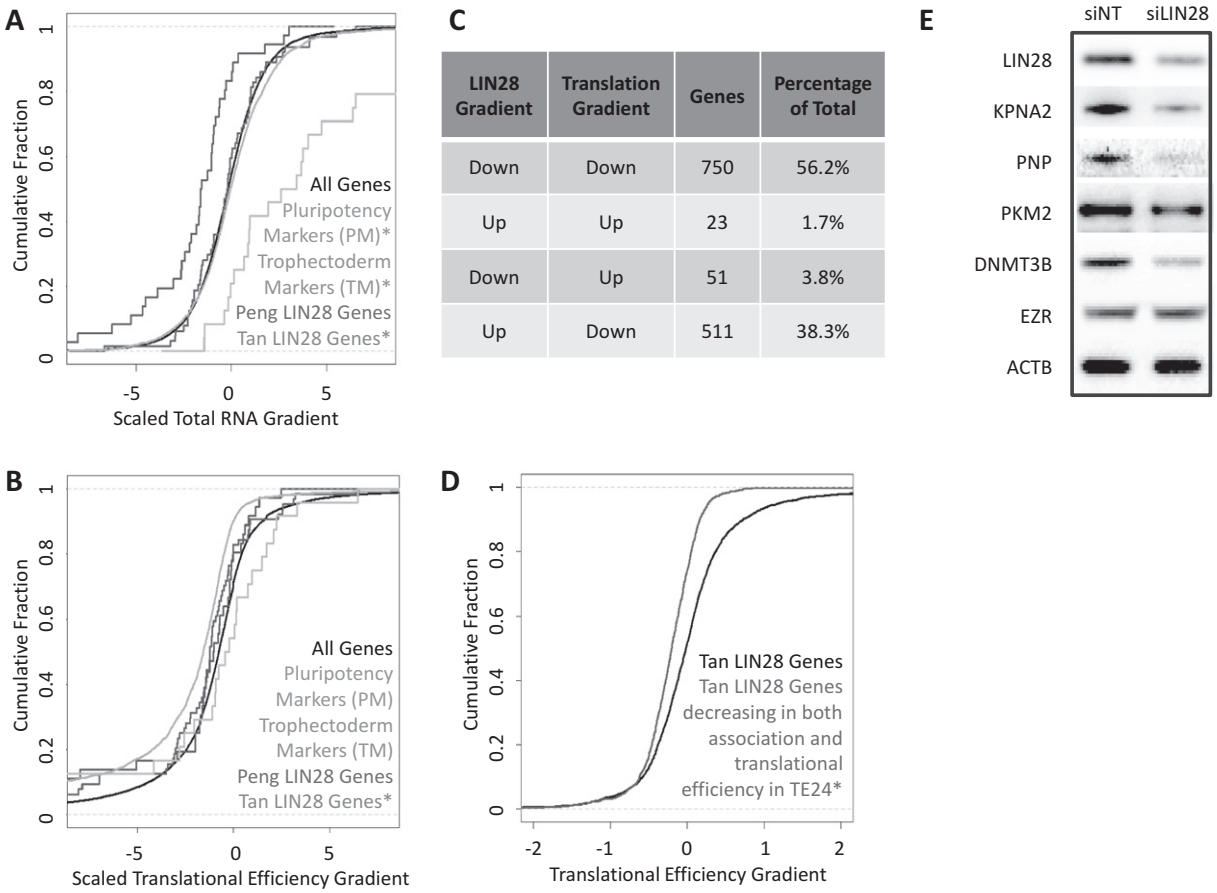

Figure 3. Gradient analysis of total RNA and translational efficiency upon differentiation. Cumulative distribution plots of (**A**) scaled total RNA gradient and (**B**) scaled translational efficiency gradient for hESCs undergoing 24 h of trophoblast differentiation. A positive gradient indicates that a particular gene is increasing in either mRNA expression (A), or translational efficiency (B). K-S tests identified significant differences between 'all genes' (black) and 'pluripotency marker' (blue) or 'trophectoderm marker' (green) genes for total RNA in (A), and between 'all genes' (black) and 'Tan LIN28 genes' (orange) for translational efficiency in (B), denoted by * p-value < 0.001. (**C**) Statistics of genes significantly changing in either LIN28 association or translational efficiency upon T24 differentiation. A large proportion of genes are significantly decreased in both LIN28 association and translational efficiency. (**D**) Cumulative distribution plot of LIN28-association gradient for hESCs undergoing neural differentiation (N24). All genes associated with LIN28 (black) were significantly different from genes that are both decreasing in association with LIN28 and decreasing in translational efficiency upon T24 (red), showing that these genes are also decreasing in LIN28 association upon N24 differentiation. * denotes a K-S test p-value of < 0.001. (**E**) Representative western blots comparing non-targeting siRNA control-transfected (siNT) to siLIN28-transfected (siLIN28) hESCs at 72 h. ACTB was used as a loading control, while EZR was a non-LIN28-associating control.

LIN28 association and translational efficiency upon differentiation (Figure 3C). Analysis of hESCs induced to differentiate with the neural protocol showed a similar pattern of response to trophoblast differentiation (Figure 3D). Of all the LIN28 mRNA cargoes identified in this study, 66% shift in a similar fashion upon induction of differentiation with either protocol (Supplementary Table S1), including novel stem cell-related targets such as *L1TD1*, *PKM2, ID1*, *PIN1* and *CSE1L*. Western blot analysis of siRNA-transfected hESCs showed that perturbation of LIN28 levels lead to decreases in protein levels of PKM2, KPNA2, PNP and DNMT3B, but not ACTB and non-LIN28-associating control EZR (Figure 3E). This pattern in protein level changes was also observed during differentiation (data not shown), where LIN28 and polysome associations with these mRNAs were shown to be decreased. These data suggest that the modulation in translational efficiency due to changes in association of LIN28 with these transcripts are specific to the loss of pluripotency, rather than the method of differentiation induction.

A gene ontology and pathway analysis of the subset of transcripts that decreased in both LIN28 association and translational efficiency upon trophoblast differentiation revealed significant enrichment in the Wnt signaling, cell cycle, RNA metabolism and proteasomal pathways (Figure 4A). By comparison, targets that increased in LIN28 association but decreased in translational efficiency upon differentiation were enriched for NGF, TNF-α/NF-κβ and IL-2 signaling pathways (Figure 4B). This implies that LIN28 binding leads to the translational enhancement and suppression of different subsets of transcripts, and corroborates a recent study in mice describing LIN28 as both a suppressor of ER-associated translation and a translational enhancer for a different set of mRNAs (25). A functional network constructed from the LIN28-associated, pathway-enriched genes in Figure 4A reveals a core set of

A

Pathway	*P*-value	Number of Genes	Percentage in Pathway
Proteasome (KEGG)	1.7 E-9	12	26.7%
Signaling by Wnt (Reactome)	2.0 E-12	17	26.6%
Cell Cycle Checkpoints (Reactome)	6.2 E-12	22	18.8%
Metabolism of RNA (Reactome)	1.3 E-9	23	14.0%
Cell Cycle Mitotic (Reactome)	1.5 E-10	35	11.1%

B

Pathway	*P*-value	Number of Genes	Percentage in Pathway
IL-2 Signaling Pathway (Wikipathways)	4.1 E-5	8	10.4%
TNF-α/NF-kβ Signaling Pathway (Wikipathways)	1.5 E-5	14	7.4%
Signaling by NGF (Reactome)	6.2 E-6	16	7.3%
RNA transport (KEGG)	1.2 E-4	11	7.2%
Pathways in cancer (KEGG)	9.6 E-5	18	5.5%

Figure 4. Gene ontology analysis of LIN28-association and translational efficiency upon differentiation. (**A**) The top five pathways for the genes that significantly decreased in both LIN28 association and translational efficiency upon differentiation. (**B**) The top five pathways for genes that are increasing in LIN28-association gradient and decreasing in translational efficiency gradient.

proteasome-related genes that are common for all pathways for trophectoderm differentiation (Figure 5). Importantly, of the 69 genes in this network that includes 15 proteasomal genes, 60 (including 14 proteasomal genes) were also decreased in LIN28-association upon neural differentiation (Supplementary Table S1). The identification of these early-response translationally regulated pathways suggests that LIN28 plays a far larger role during the initiation of differentiation, as well as control of pluripotency, than previously appreciated.

DISCUSSION

We have developed the sensitive eRIP method to track the dynamic changes of transcripts associated with endogeneous LIN28, and demonstrated that 95% of these also decrease in translational efficiency upon the onset of differentiation in hESCs. We show that the majority of transcripts that decrease in association with LIN28 also decrease in translational efficiency, and provide evidence that LIN28 controls crucial cell cycle and RNA metabolism pathways via post-transcriptional regulation of a core set of proteasome genes. Importantly, these events are captured prior to any changes in mature *let-7* miRNA levels, supporting the observation in *C. elegans* development that *let-7*-independent regulation by LIN28 occurs before *let-7*-dependent steps (19). Of the 2995 transcripts that are associated with LIN28 in this study, only a small number changed significantly in transcript expression upon differentiation, 26 with TE24 treatment and 7 with N24 treatment. This suggests that most LIN28-associated mRNAs are post-transcriptionally regulated, at least during the first 24 h of differentiation. The reproducible pattern of LIN28-associated mRNAs in undifferentiated hESCs and the rapid changes in LIN28 mRNA cargoes upon the onset of differentiation offers the potential for development of useful eRIP-based in-process or release specifications assay to test the functional quality of pluripotent stem cells destined for therapeutic use. It is envisaged that this technology could be linked to a real-time PCR detection step where a narrow gene set would be used to assess pluripotency before, or even after, differentiation.

Importantly, our eRIP method identified novel LIN28-associated transcripts. Those identified include *L1TD1*, a LIN28-interacting RBP required for hESC self-renewal (46), *PKM2*, which interacts with OCT4 and is enriched in hESCs, facilitating self-renewal and proliferation (47), as well as *ID1* and *PIN1*, critical factors for self-renewal and maintenance of pluripotent stem cells (48,49). All four of these genes decrease in LIN28 association upon both differentiation treatments and translational efficiency upon TE differentiation. Interestingly, a novel target, *CSE1L*, that is essential for early embryonic growth and development (50), increases its association with LIN28 during both differentiation treatments, but decreases in translational efficiency upon TE-induced differentiation.

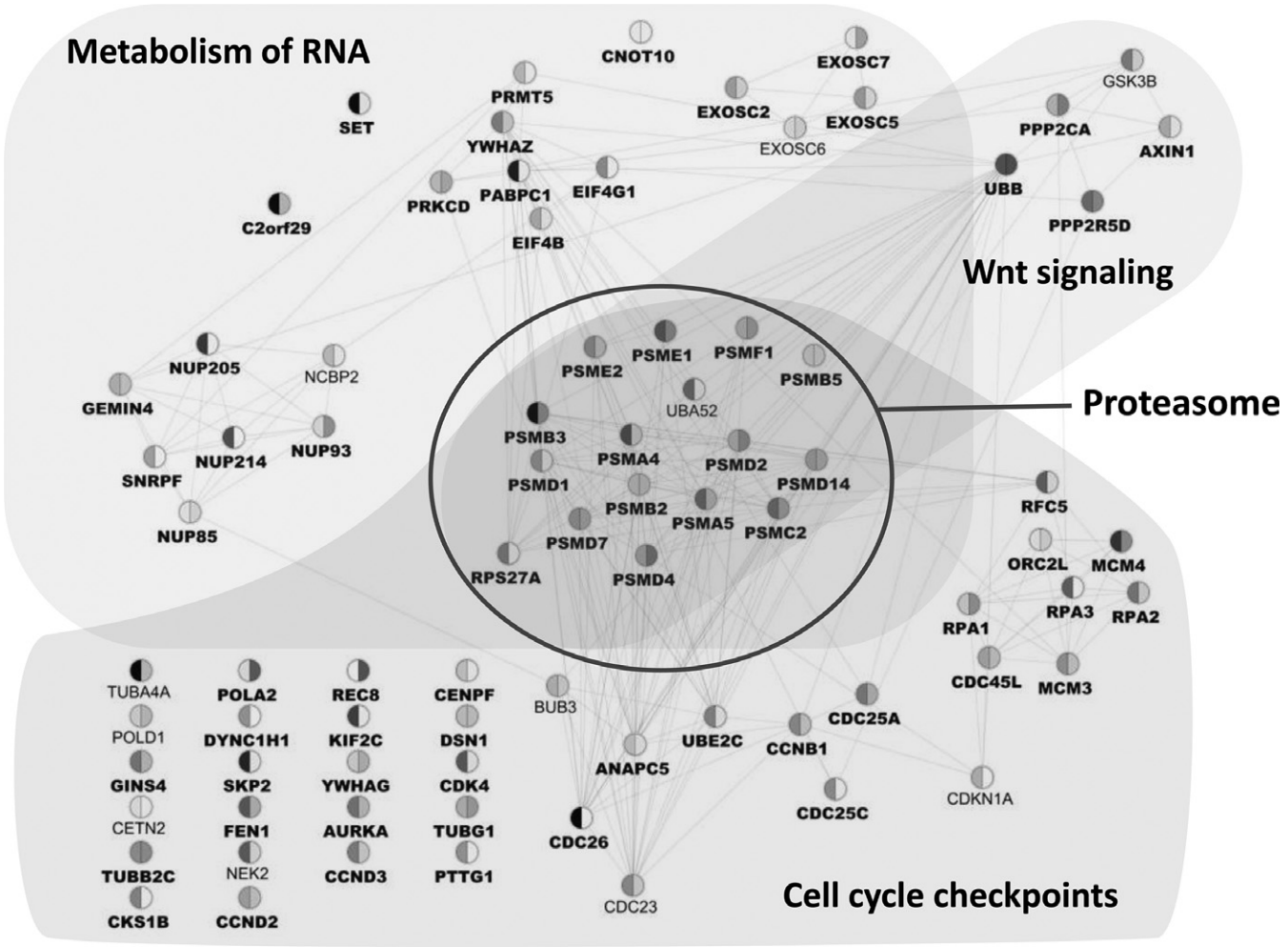

Figure 5. Network of genes that decrease in both LIN28-association and translational efficiency upon differentiation. Functional interaction network of genes in the top five pathways in Figure 4A. Each gene is represented by two semi-circles: the one on the left represents the LIN28-association gradient, and the one on the right represents the translational efficiency gradient, where white is 0 and black is −1. Genes in bold indicate a negative LIN28-association gradient upon hESC differentiation with both trophoblast and neural differentiation protocols.

The majority of the transcripts decreasing in both LIN28 association and translational efficiency include those in known LIN28-regulated pathways such as cell cycle and RNA metabolism (9,21). Downregulation of LIN28 has been shown to be important in hESC differentiation (51). Given the essential role of the Wnt signaling pathway in the maintenance of hESC pluripotency (52), it is intriguing that our data suggest that LIN28 regulates the initiation of differentiation through post-transcriptional downregulation of Wnt pathway genes. Of significance is the identification of the proteasome pathway as a central node in our analysis. Studies have shown that the proteasome is important for the maintenance of pluripotency; it is also commonly overexpressed in human mature oocytes and hESCs, and downregulated upon differentiation (53,54).

Recent work shows that LIN28 also functions as a translational repressor for ER-associated genes (25). This phenomenon is reflected in our dataset, where the genes of three signaling pathways are increasingly associated with LIN28 but decrease in translational efficiency upon hESC differentiation. Interestingly, decreased expression of NF-κβ pathway genes has been detected in differentiating hESCs (55), while IL-2 and NGF have been used to induce differentiation of hESCs to natural killer cells and neurons, respectively (56,57), lineages that are distinctly different from the trophectoderm. As the ER orchestrates the production of membrane-bound and secreted proteins, which are encoded by many genes involved in signaling pathways, it is possible that LIN28 localization to the ER alters its role in post-transcriptional regulation such that increased association with LIN28 induces decreased translation. As LIN28 levels do not change upon the initiation of differentiation, it is likely that distinct partner RBPs and/or non-coding RNAs (ncRNAs) associate with LIN28-bound transcripts, as exemplified by *BC1*-FMRP (58). Similar to the theory of eukaryotic post-transcriptional operons (59), these LIN28-associated mRNPs can recruit different factors to enhance translational efficiency, for example RNA helicase A as shown previously (20). Alternatively, RBPs such as CUGBP2, which has been shown to stabilize COX2 mRNA while suppressing its translation (60), could be recruited to LIN28-associated mRNPs. This hypothesis fits observa-

tions that LIN28 can stabilize mRNAs (41), as well as induce translational inhibition (25). It will therefore be interesting to perform LIN28 eRIP, coupled with mass spectrometric analysis, to identify the protein-interacting partners in these mRNPs.

We have demonstrated that LIN28 is a key translational determinant of the initiation of hESC differentiation. Although most of the LIN28-associated transcripts do not change in abundance upon differentiation, almost all decrease in translational efficiency, whereas only close to two-thirds decrease in LIN28-association, as revealed by eRIP and polysome analyses. Pathways important for this process include *Wnt* signaling, cell cycle and RNA metabolism, which are connected by a central proteasome core. Our data thus suggest that in the pluripotent state, LIN28 acts to sustain the translational efficiency of its target genes through contrasting mechanisms, possibly by co-association with additional RBPs or ncRNAs.

SUPPLEMENTARY DATA

Supplementary Data are available at NAR Online.

ACKNOWLEDGMENTS

The authors would like to acknowledge support by the Agency for Science, Technology and Research (A*STAR), National University of Singapore Tissue Engineering Programme, Life Science Institute, Singapore, and Curtin University, Western Australia.

FUNDING

Singapore Stem Cell Consortium [SSCC-06-006 to A.T. and R.L.]. Funding for open access charge: Curtin University.
Conflict of interest statement. None declared.

REFERENCES

1. Moss,E.G., Lee,R.C. and Ambros,V. (1997) The cold shock domain protein LIN-28 controls developmental timing in *C. elegans* and is regulated by the lin-4 RNA. *Cell*, **88**, 637–646.
2. Zhu,H., Shah,S., Shyh-Chang,N., Shinoda,G., Einhorn,W.S., Viswanathan,S.R., Takeuchi,A., Grasemann,C., Rinn,J.L., Lopez,M.F. *et al.* (2010) Lin28a transgenic mice manifest size and puberty phenotypes identified in human genetic association studies. *Nat. Genet.*, **42**, 626–630.
3. Shinoda,G., Shyh-Chang,N., Soysa,T.Y., Zhu,H., Seligson,M.T., Shah,S.P., Abo-Sido,N., Yabuuchi,A., Hagan,J.P., Gregory,R.I. *et al.* (2013) Fetal deficiency of lin28 programs life-long aberrations in growth and glucose metabolism. *Stem Cells*, **31**, 1563–1573.
4. Moss,E.G. and Tang,L. (2003) Conservation of the heterochronic regulator Lin-28, its developmental expression and microRNA complementary sites. *Dev. Biol.*, **258**, 432–442.
5. Yang,D.H. and Moss,E.G. (2003) Temporally regulated expression of Lin-28 in diverse tissues of the developing mouse. *Gene Expr. Patterns*, **3**, 719–726.
6. Richards,M., Tan,S.P., Tan,J.H., Chan,W.K. and Bongso,A. (2004) The transcriptome profile of human embryonic stem cells as defined by SAGE. *Stem Cells*, **22**, 51–64.
7. Yu,J., Vodyanik,M.A., Smuga-Otto,K., Antosiewicz-Bourget,J., Frane,J.L., Tian,S., Nie,J., Jonsdottir,G.A., Ruotti,V., Stewart,R. *et al.* (2007) Induced pluripotent stem cell lines derived from human somatic cells. *Science*, **318**, 1917–1920.
8. Tanabe,K., Nakamura,M., Narita,M., Takahashi,K. and Yamanaka,S. (2013) Maturation, not initiation, is the major roadblock during reprogramming toward pluripotency from human fibroblasts. *Proc. Natl. Acad. Sci. U.S.A.*, **110**, 12172–12179.
9. Balzer,E. and Moss,E.G. (2007) Localization of the developmental timing regulator Lin28 to mRNP complexes, P-bodies and stress granules. *RNA Biol.*, **4**, 16–25.
10. Heo,I., Joo,C., Cho,J., Ha,M., Han,J. and Kim,V.N. (2008) Lin28 mediates the terminal uridylation of let-7 precursor MicroRNA. *Mol. Cell*, **32**, 276–284.
11. Viswanathan,S.R., Daley,G.Q. and Gregory,R.I. (2008) Selective blockade of microRNA processing by Lin28. *Science*, **320**, 97–100.
12. Newman,M.A., Thomson,J.M. and Hammond,S.M. (2008) Lin-28 interaction with the Let-7 precursor loop mediates regulated microRNA processing. *RNA*, **14**, 1539–1549.
13. Piskounova,E., Viswanathan,S.R., Janas,M., LaPierre,R.J., Daley,G.Q., Sliz,P. and Gregory,R.I. (2008) Determinants of microRNA processing inhibition by the developmentally regulated RNA-binding protein Lin28. *J. Biol. Chem.*, **283**, 21310–21314.
14. Rybak,A., Fuchs,H., Smirnova,L., Brandt,C., Pohl,E.E., Nitsch,R. and Wulczyn,F.G. (2008) A feedback loop comprising lin-28 and let-7 controls pre-let-7 maturation during neural stem-cell commitment. *Nat. Cell Biol.*, **10**, 987–993.
15. Roush,S. and Slack,F.J. (2008) The let-7 family of microRNAs. *Trends Cell Biol.*, **18**, 505–516.
16. Melton,C., Judson,R.L. and Blelloch,R. (2010) Opposing microRNA families regulate self-renewal in mouse embryonic stem cells. *Nature*, **463**, 621–626.
17. Viswanathan,S.R. and Daley,G.Q. (2010) Lin28: a microRNA regulator with a macro role. *Cell*, **140**, 445–449.
18. Balzer,E., Heine,C., Jiang,Q., Lee,V.M. and Moss,E.G. (2010) LIN28 alters cell fate succession and acts independently of the let-7 microRNA during neurogliogenesis in vitro. *Development*, **137**, 891–900.
19. Vadla,B., Kemper,K., Alaimo,J., Heine,C. and Moss,E.G. (2012) Lin-28 controls the succession of cell fate choices via two distinct activities. *PLoS Genet.*, **8**, e1002588.
20. Jin,J., Jing,W., Lei,X.X., Feng,C., Peng,S., Boris-Lawrie,K. and Huang,Y. (2011) Evidence that Lin28 stimulates translation by recruiting RNA helicase A to polysomes. *Nucleic Acids Res.*, **39**, 3724–3734.
21. Peng,S., Chen,L.L., Lei,X.X., Yang,L., Lin,H., Carmichael,G.G. and Huang,Y. (2010) Genome-wide studies reveal that Lin28 enhances the translation of genes important for growth and survival of human embryonic stem cells. *Stem Cells*, **29**, 496–504.
22. Xu,B., Zhang,K. and Huang,Y. (2009) Lin28 modulates cell growth and associates with a subset of cell cycle regulator mRNAs in mouse embryonic stem cells. *RNA*, **15**, 357–361.
23. Wilbert,M.L., Huelga,S.C., Kapeli,K., Stark,T.J., Liang,T.Y., Chen,S.X., Yan,B.Y., Nathanson,J.L., Hutt,K.R., Lovci,M.T. *et al.* (2012) LIN28 binds messenger RNAs at GGAGA motifs and regulates splicing factor abundance. *Mol. Cell*, **48**, 195–206.
24. Shyh-Chang,N., Zhu,H., Yvanka de Soysa,T., Shinoda,G., Seligson,M.T., Tsanov,K.M., Nguyen,L., Asara,J.M., Cantley,L.C. and Daley,G.Q. (2013) Lin28 enhances tissue repair by reprogramming cellular metabolism. *Cell*, **155**, 778–792.
25. Cho,J., Chang,H., Kwon,S.C., Kim,B., Kim,Y., Choe,J., Ha,M., Kim,Y.K. and Kim,V.N. (2012) LIN28A is a suppressor of ER-associated translation in embryonic stem cells. *Cell*, **151**, 765–777.
26. Penalva,L.O., Burdick,M.D., Lin,S.M., Sutterluety,H. and Keene,J.D. (2004) RNA-binding proteins to assess gene expression states of co-cultivated cells in response to tumor cells. *Mol. Cancer*, **3**, 24.
27. Keene,J.D., Komisarow,J.M. and Friedersdorf,M.B. (2006) RIP-Chip: the isolation and identification of mRNAs, microRNAs and protein components of ribonucleoprotein complexes from cell extracts. *Nat. Protoc.*, **1**, 302–307.
28. Kilburn,D., Roh,J.H., Guo,L., Briber,R.M. and Woodson,S.A. (2010) Molecular crowding stabilizes folded RNA structure by the excluded volume effect. *J. Am. Chem. Soc.*, **132**, 8690–8696.
29. Lareu,R.R., Harve,K.S. and Raghunath,M. (2007) Emulating a crowded intracellular environment in vitro dramatically improves RT-PCR performance. *Biochem. Biophys. Res. Commun.*, **363**, 171–177.
30. Xu,R.H., Sampsell-Barron,T.L., Gu,F., Root,S., Peck,R.M., Pan,G., Yu,J., Antosiewicz-Bourget,J., Tian,S., Stewart,R. *et al.* (2008)

NANOG is a direct target of TGFbeta/activin-mediated SMAD signaling in human ESCs. *Cell Stem Cell*, **3**, 196–206.
31. Christie,V.B., Barnard,J.H., Batsanov,A.S., Bridgens,C.E., Cartmell,E.B., Collings,J.C., Maltman,D.J., Redfern,C.P., Marder,T.B., Przyborski,S. *et al.* (2008) Synthesis and evaluation of synthetic retinoid derivatives as inducers of stem cell differentiation. *Org. Biomol. Chem.*, **6**, 3497–3507.
32. Soh,B.S., Song,C.M., Vallier,L., Li,P., Choong,C., Yeo,B.H., Lim,E.H., Pedersen,R.A., Yang,H.H., Rao,M. *et al.* (2007) Pleiotrophin enhances clonal growth and long-term expansion of human embryonic stem cells. *Stem Cells*, **25**, 3029–3037.
33. Tay,Y.M., Tam,W.L., Ang,Y.S., Gaughwin,P.M., Yang,H., Wang,W., Liu,R., George,J., Ng,H.H., Perera,R.J. *et al.* (2008) MicroRNA-134 modulates the differentiation of mouse embryonic stem cells, where it causes post-transcriptional attenuation of Nanog and LRH1. *Stem Cells*, **26**, 17–29.
34. Zhang,D., Zhao,T., Ang,H.S., Chong,P., Saiki,R., Igarashi,K., Yang,H. and Vardy,L.A. (2012) AMD1 is essential for ESC self-renewal and is translationally down-regulated on differentiation to neural precursor cells. *Genes Dev.*, **26**, 461–473.
35. Swartz,J.E., Bor,Y.C., Misawa,Y., Rekosh,D. and Hammarskjold,M.L. (2007) The shuttling SR protein 9G8 plays a role in translation of unspliced mRNA containing a constitutive transport element. *J. Biol. Chem.*, **282**, 19844–19853.
36. Chua,S.W., Vijayakumar,P., Nissom,P.M., Yam,C.Y., Wong,V.V. and Yang,H. (2006) A novel normalization method for effective removal of systematic variation in microarray data. *Nucleic Acids Res.*, **34**, e38.
37. Montojo,J., Zuberi,K., Rodriguez,H., Kazi,F., Wright,G., Donaldson,S.L., Morris,Q. and Bader,G.D. (2010) GeneMANIA Cytoscape plugin: fast gene function predictions on the desktop. *Bioinformatics*, **26**, 2927–2928.
38. Cline,M.S., Smoot,M., Cerami,E., Kuchinsky,A., Landys,N., Workman,C., Christmas,R., Avila-Campilo,I., Creech,M., Gross,B. *et al.* (2007) Integration of biological networks and gene expression data using Cytoscape. *Nat. Protoc.*, **2**, 2366–2382.
39. Smyth,G.K. (2004) Linear models and empirical bayes methods for assessing differential expression in microarray experiments. *Stat. Appl. Genet. Mol. Biol.*, **3**, 3.
40. Kikin,O., D'Antonio,L. and Bagga,P.S. (2006) QGRS Mapper: a web-based server for predicting G-quadruplexes in nucleotide sequences. *Nucleic Acids Res.*, **34**, W676–W682.
41. Hafner,M., Max,K.E., Bandaru,P., Morozov,P., Gerstberger,S., Brown,M., Molina,H. and Tuschl,T. (2013) Identification of mRNAs bound and regulated by human LIN28 proteins and molecular requirements for RNA recognition. *RNA*, **19**, 613–626.
42. Ramos,A., Hollingworth,D. and Pastore,A. (2003) G-quartet-dependent recognition between the FMRP RGG box and RNA. *RNA*, **9**, 1198–1207.
43. Mukherjee,N., Corcoran,D.L., Nusbaum,J.D., Reid,D.W., Georgiev,S., Hafner,M., Ascano,M. Jr, Tuschl,T., Ohler,U. and Keene,J.D. (2011) Integrative regulatory mapping indicates that the RNA-binding protein HuR couples pre-mRNA processing and mRNA stability. *Mol. Cell*, **43**, 327–339.
44. Sampath,P., Pritchard,D.K., Pabon,L., Reinecke,H., Schwartz,S.M., Morris,D.R. and Murry,C.E. (2008) A hierarchical network controls protein translation during murine embryonic stem cell self-renewal and differentiation. *Cell Stem Cell*, **2**, 448–460.
45. Marchand,M., Horcajadas,J.A., Esteban,F.J., McElroy,S.L., Fisher,S.J. and Giudice,L.C. (2011) Transcriptomic signature of trophoblast differentiation in a human embryonic stem cell model. *Biol. Reprod.*, **84**, 1258–1271.
46. Narva,E., Rahkonen,N., Emani,M.R., Lund,R., Pursiheimo,J.P., Nasti,J., Autio,R., Rasool,O., Denessiouk,K., Lahdesmaki,H. *et al.* (2012) RNA-binding protein L1TD1 interacts with LIN28 via RNA and is required for human embryonic stem cell self-renewal and cancer cell proliferation. *Stem Cells*, **30**, 452–460.
47. Lee,J., Kim,H.K., Han,Y.M. and Kim,J. (2008) Pyruvate kinase isozyme type M2 (PKM2) interacts and cooperates with Oct-4 in regulating transcription. *Int. J. Biochem. Cell Biol.*, **40**, 1043–1054.
48. Romero-Lanman,E.E., Pavlovic,S., Amlani,B., Chin,Y. and Benezra,R. (2012) Id1 maintains embryonic stem cell self-renewal by up-regulation of Nanog and repression of Brachyury expression. *Stem Cells Dev.*, **21**, 384–393.
49. Nishi,M., Akutsu,H., Masui,S., Kondo,A., Nagashima,Y., Kimura,H., Perrem,K., Shigeri,Y., Toyoda,M., Okayama,A. *et al.* (2011) A distinct role for Pin1 in the induction and maintenance of pluripotency. *J. Biol. Chem.*, **286**, 11593–11603.
50. Bera,T.K., Bera,J., Brinkmann,U., Tessarollo,L. and Pastan,I. (2001) Cse1l is essential for early embryonic growth and development. *Mol. Cell Biol.*, **21**, 7020–7024.
51. Darr,H. and Benvenisty,N. (2009) Genetic analysis of the role of the reprogramming gene LIN-28 in human embryonic stem cells. *Stem Cells*, **27**, 352–362.
52. Sato,N., Meijer,L., Skaltsounis,L., Greengard,P. and Brivanlou,A.H. (2004) Maintenance of pluripotency in human and mouse embryonic stem cells through activation of Wnt signaling by a pharmacological GSK-3-specific inhibitor. *Nat. Med.*, **10**, 55–63.
53. Assou,S., Cerecedo,D., Tondeur,S., Pantesco,V., Hovatta,O., Klein,B., Hamamah,S. and De Vos,J. (2009) A gene expression signature shared by human mature oocytes and embryonic stem cells. *BMC Genomics*, **10**, 10.
54. Vilchez,D., Boyer,L., Morantte,I., Lutz,M., Merkwirth,C., Joyce,D., Spencer,B., Page,L., Masliah,E., Berggren,W.T. *et al.* (2012) Increased proteasome activity in human embryonic stem cells is regulated by PSMD11. *Nature*, **489**, 304–308.
55. Armstrong,L., Hughes,O., Yung,S., Hyslop,L., Stewart,R., Wappler,I., Peters,H., Walter,T., Stojkovic,P., Evans,J. *et al.* (2006) The role of PI3K/AKT, MAPK/ERK and NFkappabeta signalling in the maintenance of human embryonic stem cell pluripotency and viability highlighted by transcriptional profiling and functional analysis. *Hum. Mol. Genet.*, **15**, 1894–1913.
56. Woll,P.S., Grzywacz,B., Tian,X., Marcus,R.K., Knorr,D.A., Verneris,M.R. and Kaufman,D.S. (2009) Human embryonic stem cells differentiate into a homogeneous population of natural killer cells with potent in vivo antitumor activity. *Blood*, **113**, 6094–6101.
57. Schuldiner,M., Eiges,R., Eden,A., Yanuka,O., Itskovitz-Eldor,J., Goldstein,R.S. and Benvenisty,N. (2001) Induced neuronal differentiation of human embryonic stem cells. *Brain Res.*, **913**, 201–205.
58. Lacoux,C., Di Marino,D., Boyl,P.P., Zalfa,F., Yan,B., Ciotti,M.T., Falconi,M., Urlaub,H., Achsel,T., Mougin,A. *et al.* (2012) BC1-FMRP interaction is modulated by 2'-O-methylation: RNA-binding activity of the tudor domain and translational regulation at synapses. *Nucleic Acids Res.*, **40**, 4086–4096.
59. Keene,J.D. and Tenenbaum,S.A. (2002) Eukaryotic mRNPs may represent posttranscriptional operons. *Mol. Cell*, **9**, 1161–1167.
60. Mukhopadhyay,D., Houchen,C.W., Kennedy,S., Dieckgraefe,B.K. and Anant,S. (2003) Coupled mRNA stabilization and translational silencing of cyclooxygenase-2 by a novel RNA binding protein, CUGBP2. *Mol. Cell*, **11**, 113–126.